Chapter 8
Cyclic Plasticity Models: Critical Reviews and Assessments

Accurate description of plastic deformation induced during a cyclic loading process is required for the mechanical design of machinery subjected to vibration and buildings and soil structures subjected to earthquakes since the middle of the last century. Elastoplastic constitutive model formulated for this aim is called the *cyclic plasticity model*. Substantially, the key of the pertinence in cyclic plasticity model is how to describe appropriately a small plastic strain rate induced by the rate of stress inside the yield surface. Therefore, a quite delicate formulation of plastic strain rate developing gradually as the stress approaches the yield surface is required to this end. Here, needless to say, the continuity and the smoothness conditions described in Sect. 7.1 would have to be fulfilled in a cyclic plasticity model.

Various cyclic plasticity models have been proposed to date, while most of them violate the continuity and the smoothness conditions unfortunately. Then, the beginners for the cyclic plasticity model would be perplexed as to which model is most pertinent and should be chosen for their study and analyses. In order to avoid their perplexity and missed selections, the cyclic plasticity models will be classified from the mathematical structures and their distinctive physical features will be examined in this chapter. Then, their pertinences/impertinences will be critically assessed in detail.

8.1 Classification of Cyclic Plasticity Models

Cyclic plasticity models proposed to date are classifiable into the two types described in the following.

K. Hashiguchi, *Foundations of Elastoplasticity: Subloading Surface Model*,
DOI 10.1007/978-3-319-48821-9_8

The one type is based on the concept of the kinematic hardening, i.e., the translation of subyield surface(s) assumed inside the conventional yield surface or the small single yield surface translating rapidly with a plastic deformation, while the innermost surface encloses a purely elastic domain. Several cyclic plasticity models in this type have been proposed to date. The other type is based on the natural concept that the plastic strain rate develops as the stress approaches the yield surface, i.e. the extension of the subloading surface model described in Chap. 7. The cyclic loading behavior is described rigorously by extending the subloading surface model such that the similarity-center of the normal-yield and the subloading surfaces translates with the plastic deformation. It is called the *extended subloading surface model*, while the subloading surface model described in Chap. 7 for which the similarity-center is fixed is renamed the *initial subloading surface model*.

The classification of the cyclic plasticity models is shown schematically in Fig. 8.1. Their mathematical and mechanical features and pertinences/impertinences to the description of cyclic loading behavior will be revealed in detail in the subsequent sections.

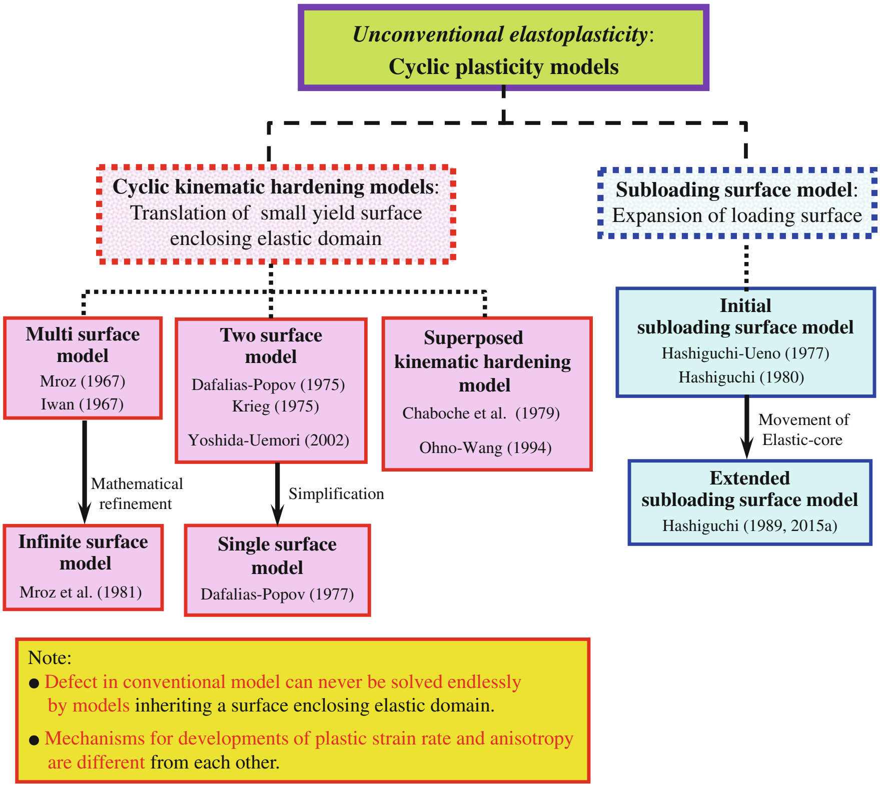

Fig. 8.1 Classification of cyclic plasticity models

8.2 Cyclic Kinematic Hardening Models: Improper Use of Kinematic Hardening

The conventional plasticity postulates that a plastic strain rate is induced by the rate of stress on the yield surface but it is required for the cyclic plasticity model to describe the plastic strain rate induced by the rate of stress inside the yield surface. The description of plastic deformation induced in the cyclic loading process was initiated by exploiting the kinematic hardening concept with the assumption of existence of a purely elastic domain. It is called the *cyclic kinematic hardening model*. However, we should notice the following crucial defects.

1. The stress region, in which a plastic strain rate is not induced but only an elastic strain rate is induced by cyclic change of stress, does not exist in general as known from the fact that the plastic strain rate is induced during a cyclic loading with any small stress amplitude. Therefore, the yield surface enclosing a purely-elastic domain must not be incorporated in the modelling of cyclic elastoplastic constitutive equation.
2. The purpose for the creation of unconventional plasticity model is the description of the plastic strain rate by the rate of stress inside the yield surface which cannot be described by the conventional plasticity model assuming the yield surface enclosing a purely-elastic domain. However, the cyclic kinematic hardening models are incapable of describing the plastic strain rate in the cyclic loading by the stress amplitude inside the small yield surface enclosing a purely-elastic domain. Then, the models inheriting the yield surface enclosing a purely-elastic domain are required to incorporate smaller and smaller yield surfaces one after another endlessly depending on the stress level and the stress amplitude, like an infinity mirror, a nest of boxes, a matryoshka doll in Russia, etc. so that they fall into the endless pit without the fundamental resolution of the problem. In addition, note that it cannot be physically accepted to incorporate an infinitely small yield surface, resulting in the indetermination of the direction of plastic strain rate, since the normal direction to the infinitesimal surface is indeterminate. Eventually, ***the defect of the conventional plasticity model cannot be solved by the cyclic kinematic hardening models*** inheriting a (small) yield surface enclosing a purely-elastic domain.
3. The ***mechanism for the development of plastic strain rate is substantially different from the mechanism for the development of anisotropy*** such as the kinematic hardening,
4. A purely elastic state would not move up to a high stress in a fully-yield state.
5. Plastic deformation behavior of material with a fatigue limit smaller than a size of yield surface enclosing a purely-elastic domain cannot be described for the stress amplitude smaller than the size of yield surface.

Besides, remind that the kinematic hardening (Prager 1956; Armstrong and Frederick 1966) is merely the simple method proposed primarily to describe the induced anisotropy of non-frictional, i.e. plastically-pressure independent metals.

The kinematic hardening is inapplicable but the rotational hardening rule (cf. Chap. 11) has to be adopted to describe the anisotropy of the plastically-pressure dependent, i.e. frictional materials (e.g. soils, rocks, concretes and friction behavior). The cyclic kinematic hardening models would not possess the rationality and the generality as will be explained in detail for each model.

8.2.1 Multi-surface Model

Mroz (1966, 1967, 1976) and Iwan (1967) proposed the *multi surface model* based on the following basic assumptions.

(a) Plural encircled subyield surfaces are incorporated, while the ratios of the sizes of these surfaces to the outer-most surface (conventional yield surface) are kept constant throughout a deformation.
(b) Interior of the innermost subyield surface is a purely-elastic domain.
(c) Subyield surfaces are pushed out by the current stress point. Then, plural surfaces contact at a point.
(d) Plastic modulus is prescribed by the size of the subyield surface on which the current stress lies, while it is smaller for a more outer subyield surface.

The uniaxial deformation behavior of the multi-surface model is illustrated in Fig. 8.2 for the simple material without a variation of the outmost surface.

However, this model possesses the following serious defects.

1. Plastic modulus decreases suddenly at the moment when the stress reaches a larger subyield surface, so that the smoothness condition in Eq. (7.2) is violated at that moment. Smooth stress-strain curve cannot be described but piece-wise linear curve is predicted. Therefore, it is required to determine the offset value, i.e. the plastic stain at yield point, which is accompanied with an arbitrariness.
2. Plural subyield surfaces contact at the current stress point and there exist plural plastic moduli at that contact point so that the singular point in the field of plastic modulus is induced there. Numerical calculation becomes unstable for the cyclic loading behavior in the vicinity of contact point.
3. Plastic deformation cannot be predicted at all for the cyclic loading inside the innermost surface even in a high stress level.
4. It is physically impertinent that the innermost subyield surface contacts with the outermost surface, so that the purely-elastic domain reaches the fully-plastic state.
5. Stress transfers to a larger subyield surface by moving half of the difference of the sizes of subyield surfaces in the initial loading process as shown in Fig. 8.2b. On the other hand, it transfers to a larger subyield surface by moving just the difference of the sizes of subyield surfaces in the unloading-reverse loading process as shown in Fig. 8.2d. Therefore, the *Masing rule* (Masing 1926) meaning that the curvature of stress-strain curve in the unloading-reverse loading decreases to a half of the curvature of initial loading curve is described

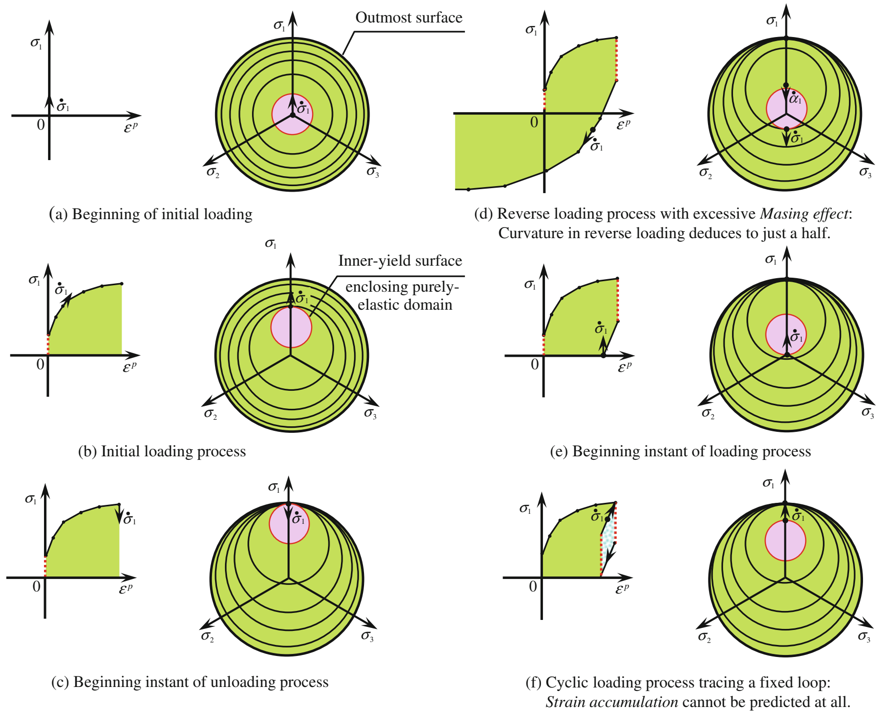

Fig. 8.2 One-dimensional loading behavior predicted by multi-surface model

exactly and simply as shown in Fig. 8.2d. By virtue of this mechanical feature, this model has been used widely. However, the variation of curvature observed in real material behavior is not so large as described by the Masing rule.

6. In the cyclic loading process under a constant amplitude, the *plastic shakedown* is induced immediately for non-hardening (sub)yield surfaces and after several cycles for hardening (sub)yield surfaces, tracing the fixed loop cyclically (Figs. 8.2f and 8.3). In other words, the accumulation of plastic strain during a pulsating stress loading, called the *mechanical ratcheting effect*, cannot be described at all by this model. In fact, however, the remarkable mechanical ratcheting is observed in real metal behavior which can be simulated accurately by the extended subloading surface model as will be described in Sect. 10.4 for metals. Therefore, the deformations of machinery and structures subjected to cyclic loading are predicted to be unrealistically small by the multi surface model, resulting in a risky mechanical design of machinery.
7. The continuity condition in Eq. (7.1) is also violated at the moment when the stress transfers to a larger subyield surface if the tangential inelastic strain rate described in Sect. 7.7 is incorporated, which is induced discontinuously.

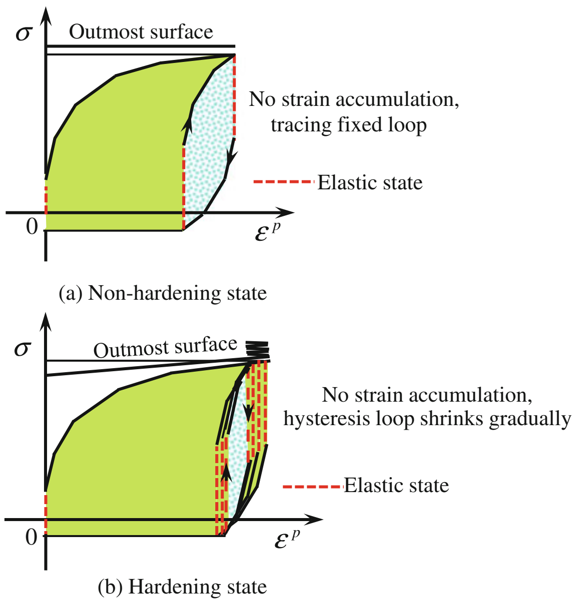

Fig. 8.3 Prediction of cyclic loading behavior by the multi surface model under a constant stress amplitude

8. Judgment on which subyield surface among multiple subyield surfaces the current stress lies is required in the loading criterion. In addition, deformation analysis by this model is complicated because it is necessary to calculate all movements of multi-subyield surfaces. It results in the increases of memory usage and calculations necessary for numerical analysis. It becomes more serious in the analysis of cyclic loading behavior in fluctuating unsteady loading process.
9. Numerical calculation of cyclic loading behavior in the vicinity of innermost yield surface is unstable, the tangent modulus jumping from the elastic to the elastoplastic ones and vice versa.

8.2.2 Infinite Surface Model

Modification of the multi surface model was proposed by Mroz et al. (1981), in which infinite number of subyield surfaces are incorporated inside the yield surface in contrast to the two surface model described in the next subsection. It is called the *infinite surface model*. The smoothness condition in Eq. (7.2) is fulfilled so that the smooth stress-strain curve is described in the initial monotonic loading process but it is violated at the moment when the stress passes through the starting point of reverse loading, called the *stress reversal point*, in the reloading process after the partial unloading, whereas the singularity of the plastic modulus is induced at that point, since subyield surfaces with different sizes contact mutually. It is caused by the inherent characteristic of the multi surface model that the plural yield surfaces contact at one point, resulting in the singularity of the plastic modulus. All the defects (1)–(9) described in the multi surface model except for (3) and the fulfillment of smoothness condition in the initial monotonic loading process are retained in the infinite surface model. Further, note that the incorporation of an infinitely small yield surface cannot be physically accepted since it causes the singularity in the direction of plastic strain rate as was described in the item 2 in Section 8.2.

8.2.3 Two-Surface Model

Dafalias and Popov (1975, 1976) and Krieg (1975) proposed the *two-surface model* based on the following assumptions:

(a) Only one subyield surface enclosing a purely-elastic domain is incorporated inside the conventional-yield surface which is renamed as the "*bounding surface*" by Dafalias and Popov (1975) and "limit surface" by Krieg (1975).
(b) The ratio of the size of the subyield surface to that of the bounding surface is kept constant throughout the deformation.
(c) The subyield surface is pushed out by the current stress point and translates toward the conjugate point on the bounding surface, while the outward-normal at conjugate point on the bounding surface is identical with that at the current stress point on the subyield surface.
(d) The plastic modulus is determined by the distance from the current stress point to the conjugate stress point on the bounding surface.

Here, it is required that the subyield surface must translate so as not to intersect with the bounding surface because the direction of plastic strain rate becomes indeterminate at the intersecting point of these surfaces. The rigorous translation rule was derived by Hashiguchi (1981, 1988).

This model has been adopted widely for the prediction of deformation behavior of metals (cf. e.g. Dafalias and Popov 1976; McDowell 1985, 1989; Ohno and Kachi 1986; Ellyin 1989; Hassan and Kyriakides 1992; Yoshida and Uemori 2002a, b, 2003).

The uniaxial loading behavior of the two-surface model is illustrated in Fig. 8.4 for the simple material without a variation of the bounding surface. The mechanical response of this model is opposite to that of the multi-surface model, although they would seem similar since only the numbers of subyield surfaces are different, as follows:

1. The tangent modulus changes suddenly from the elastic to the elastoplastic modulus at the moment when the stress reaches the subyield surface. Therefore, the smoothness condition in Eq. (7.2) is violated at that moment. Needless to say, the smooth stress-strain curve is not described but the suddenly-bent stress-strain curve is predicted. Therefore, it is required to determine the offset value, which is accompanied with an arbitrariness.

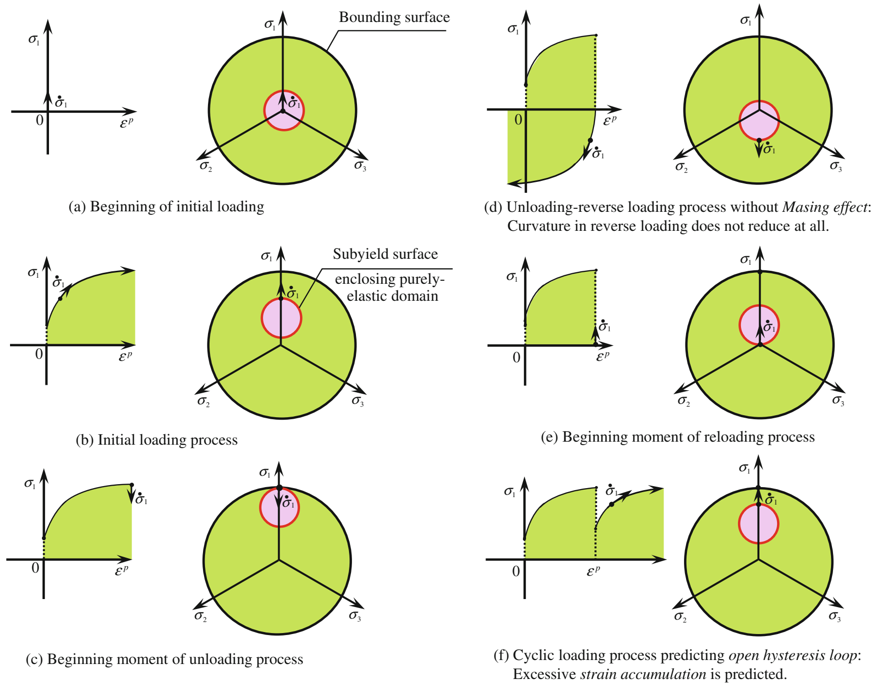

(a) Beginning of initial loading

(b) Initial loading process

(c) Beginning moment of unloading process

(d) Unloading-reverse loading process without *Masing effect*: Curvature in reverse loading does not reduce at all.

(e) Beginning moment of reloading process

(f) Cyclic loading process predicting *open hysteresis loop*: Excessive *strain accumulation* is predicted.

Fig. 8.4 Uniaxial loading behavior predicted by two-surface model

2. The *singular point* of plastic modulus is induced at the contact point of the bounding and the subyield surfaces, while the elastic and the elastoplastic tangent moduli are induced at that one point. Numerical calculation of cyclic loading behavior in the vicinity of contact point becomes unstable.
3. Plastic deformation cannot be predicted at all for the cyclic loading inside the cyclic stress inside the subyield surface even in a high stress level.
4. It is physically impertinent that the subyield surface enclosing the purely-elastic domain contacts directly with the bounding surface describing the fully-plastic state.
5. The plastic modulus depends on the distance from the current stress to the conjugate stress irrespective of the loading process, i.e. the initial, the reverse and the reloading processes and thus the curvature of stress-strain curves are identical irrespective of these processes. Then, the Masing effect cannot be described at all contrary to the multi-surface model. The ratio of the size of the inner-yield surface to that of the bounding surface is chosen to be 1/3–2/5

(Yoshida and Uemori 2002a, b, 2003) so that the inner yield surface contains the zero stress state as far as a kinematic hardening does not highly develop. Based on this fact too, it is obvious that plastic strain rate cannot be predicted in the unloading (stress reducing) process by this model and the size ratio must be chosen less than $1/4$ in order that the inner yield surface does not contain the zero stress state in general. Eventually, the unloading behavior becomes unrealistically elastic in order that the initial loading curve matches to real behavior. Consequently, the closed hysteresis loop cannot be depicted in the pulsating loading process (positive or negative one side cyclic loading process) so that the unrealistically large mechanical ratchetting is predicted. Stress versus strain curves are depicted in reloading process but unloading process have never been depicted in the pulsating loading in literatures (Yoshida and Uemori 2002a, b, 2003). Nevertheless, Yoshida and Uemori (2002a, b, 2003) insist that their model can predict the spring-back phenomenon. In their formulation, the Young's modulus is formulated to decrease but saturate to the limited value with the plastic equivalent strain in order to improve the simulation of the test data of *spring-back* behavior of metals. In fact, however, if once the Young's modulus decreases in the tension loading, it decreases acceleratingly to zero, since the decrease of the Young's modulus is caused by the growth of cracks which develop increasingly in the continuing tension loading process as has been revealed in the damage mechanics described in Chap. 14. Therefore, the method for prediction of springback due to the decrease of Young's modulus (Yoshida and Uemori 2003) is physically unacceptable, which also leads to the unrealistic prediction of deformation behavior after the springback. In other words, it would be quite irrational idea invented deceiving the inherent defect of the two surface model that only the elastic deformation is induced in the unloading (stress reducing) process as will be examined in detail in Sect. 10.5.

6. In the cyclic loading process with the constant amplitude of the positive or negative one side stress, the open hysteretic loop is described and thus the excessive strain accumulation in the cyclic loading, i.e. the excessive mechanical ratcheting is predicted contrary to the multi-surface model as shown in Fig. 8.5.
7. The continuity condition in Eq. (7.1) is also violated at the moment when the stress reaches the bounding surface if the tangential inelastic strain rate is incorporated.
8. Judgment whether or not the current stress reaches the subyield and/or the bounding surface is required in the loading criterion.
9. Numerical calculation of cyclic loading behavior in the vicinity of subyield surface is unstable, the tangent modulus jumping from the elastic to the elastoplastic ones and vice versa.

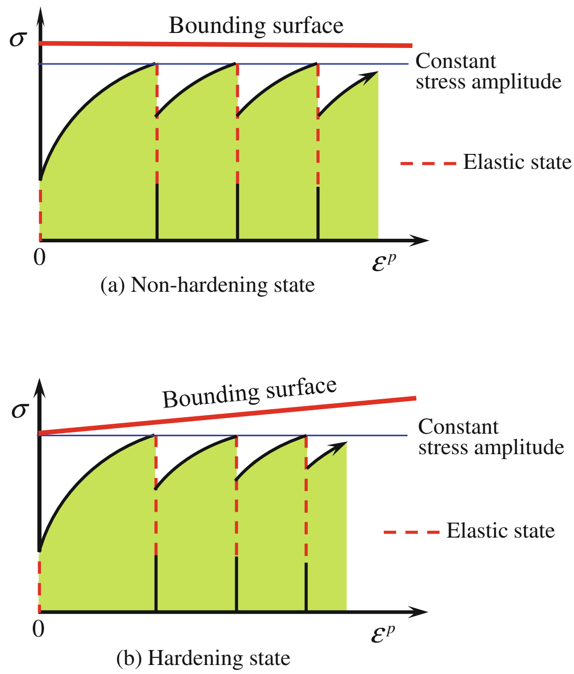

Fig. 8.5 Prediction of cyclic loading behavior by the two surface model under a constant stress amplitude

8.2.4 Single Surface Model

The *single surface model* is proposed by Dafalias and Popov (1977), in which the subyield surface shrinks to a point in the two surface model. It would describe a smooth response unless the shrinking surface does not lie on the bounding surface. Besides, the intense dependence of the direction of plastic strain rate on the direction of stress rate leading to the rate-nonlinearity which would be impertinent physically and mathematically. Further, this model cannot be free from the basic defects contained in the two-surface model.

8.2.5 Superposed Kinematic Hardening Model

The cyclic plasticity model assuming the small single yield surface which translates by the superposition of plural non-linear kinematic rules, excluding the conventional yield surface, was proposed by Chaboche et al. (1979) and Chaboche and Rousselier (1983). It may be called the *superposed kinematic hardening model.* Its alteration was proposed by Ohno and Wang (1993), which is called the *combined nonlinear kinematic-isotropic hardening model* by Ohno et al. (2013). It is not an physical model but merely an empirical model in the polynomial approximation of test data by using a lot of material constants lacking physical meanings.

(a) Chaboche model

The following small Mises type yield surface with the isotropic and the Armstrong-Frederick (1966) kinematic hardenings is introduced by Chaboche et al. (1979) and improved by Chaboche and Rousselier (1983).

$$\sqrt{\frac{3}{2}}||\hat{\boldsymbol{\sigma}}'|| = F_0 + \overline{F} \tag{8.1}$$

where the increase of the isotropic hardening function, $\bar{F}$, evolves by the following equation.

$$\dot{\overline{F}} = c(\overline{F}_s - \overline{F})\dot{\varepsilon}^{eqp} \tag{8.2}$$

c is the material constant and $\bar{F}_s$ is the material constant describing the saturation value of $\bar{F}$.

The kinematic hardening is given by the superposition of the several non-linear kinematic hardening rules of Armstrong and Frederick (1966) as follows:

$$\dot{\boldsymbol{\alpha}} = \sum_{i=1}^{n} \dot{\boldsymbol{\alpha}}_i \tag{8.3}$$

where

$$\dot{\boldsymbol{\alpha}}_i = \left(A_i \hat{\mathbf{n}} - \sqrt{\frac{2}{3}} b_i \boldsymbol{\alpha}_i \right) ||\dot{\boldsymbol{\varepsilon}}^p|| \ (\text{no sum}) \tag{8.4}$$

which is based on Eq. (6.114). A_i and b_i $(i = 1, 2, \ldots, n)$ are the material constants, while n is chosen usually $4 \sim 8$. Equation (8.3) is integrated for the uniaxial loading process as follows:

$$\alpha_a = \sum_{i=1}^{n} \frac{A_i}{b_i} [1 - \exp(-b_i \varepsilon_a^p)] \tag{8.5}$$

for $\varepsilon_a^p > 0$ under the initial condition $\alpha_a = 0$ for $\varepsilon_a^p = 0$.

The uniaxial loading behavior of Chaboche model is illustrated in Fig. 8.6, where the isotropic hardening is not incorporated by setting $c = 0$.

(b) Ohno-Wang model

Ohno and Wang (1993) introduced the small Mises type yield surface which translates by the superposition of the several bilinear kinematic hardening rules composed of the linear kinematic hardening and the isotropic non-hardening as follows:

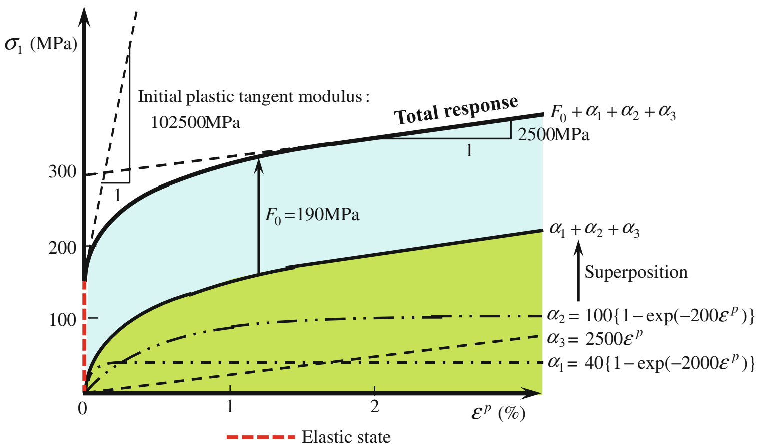

Fig. 8.6 Chaboche model (after Lamaitre and Chaboche 1990)

$$\sqrt{\frac{3}{2}}||\hat{\boldsymbol{\sigma}}'|| = F_c \tag{8.6}$$

where F_c is the material constant and thus the isotropic hardening is not induced. The kinematic hardening rule is given by

$$\dot{\boldsymbol{\alpha}} = \sum_{i=1}^{n} \dot{\boldsymbol{\alpha}}_i \tag{8.7}$$

$$\dot{\boldsymbol{\alpha}}_i = h_i\left(\frac{2}{3}\dot{\boldsymbol{\varepsilon}}^p - H[f_i]\left\langle \dot{\boldsymbol{\varepsilon}}^p : \frac{\boldsymbol{\alpha}_i}{\bar{a}_i}\right\rangle \frac{\boldsymbol{\alpha}_i}{r_i}\right) \quad \text{(no sum)} \tag{8.8}$$

where h_i and r_i $(i = 1, 2, \ldots, n)$ are the material constants, while n is chosen $4 \sim 8$ usually. The linear kinematic hardenings proceed but they stop suddenly when the following condition is satisfied in each of them.

$$f_i \equiv \bar{a}_i^2 - r_i^2 \tag{8.9}$$

where

$$\bar{a}_i \equiv \sqrt{\frac{3}{2}}||\boldsymbol{\alpha}_i|| \tag{8.10}$$

$H[\ ]$ is the Heaviside step function, i.e., $H[s] = 1$ for $s \geq 0$, $H[s] = 0$ for $s < 0$. Then, the kinematic hardening proceeds when the plastic strain rate is induced directing outwards the surface described by Eq. (8.9) but it ceases when $\boldsymbol{\alpha}_i$ reaches the surface $f_i \equiv \bar{a}_i^2 - r_i^2 = 0$ $(H[f_i] = 1)$ as ascertained by

$$
\begin{aligned}
\dot{f}_i &= 2\bar{a}_i\dot{\bar{a}}_i = 2\bar{a}_i\sqrt{\frac{3}{2}}(||\boldsymbol{\alpha}_i||)^{\bullet} = 2\bar{a}_i\sqrt{\frac{3}{2}}\frac{\boldsymbol{\alpha}_i}{||\boldsymbol{\alpha}_i||}:\overset{\circ}{\boldsymbol{\alpha}}_i \\
&= 2\bar{a}_i\sqrt{\frac{3}{2}}\frac{\boldsymbol{\alpha}_i}{||\boldsymbol{\alpha}_i||}:h_i\left(\frac{2}{3}\dot{\boldsymbol{\varepsilon}}^p - H[f_i]\left\langle \dot{\boldsymbol{\varepsilon}}^p:\frac{\boldsymbol{\alpha}_i}{\bar{a}_i}\right\rangle\frac{\boldsymbol{\alpha}_i}{r_i}\right) \\
&= 2\bar{a}_i\sqrt{\frac{3}{2}}\frac{\boldsymbol{\alpha}_i}{||\boldsymbol{\alpha}_i||}:h_i\left(\frac{2}{3}\dot{\lambda}\frac{\boldsymbol{\alpha}_i}{||\boldsymbol{\alpha}_i||} - \left\langle \dot{\lambda}\frac{\boldsymbol{\alpha}_i}{||\boldsymbol{\alpha}_i||}:\frac{\boldsymbol{\alpha}_i}{\bar{a}_i}\right\rangle\frac{\boldsymbol{\alpha}_i}{\bar{a}_i}\right) \\
&= 2\bar{a}_i\sqrt{\frac{3}{2}}\frac{\boldsymbol{\alpha}_i}{||\boldsymbol{\alpha}_i||}:h_i\left(\frac{2}{3}\dot{\lambda}\frac{\boldsymbol{\alpha}_i}{||\boldsymbol{\alpha}_i||} - \left\langle \dot{\lambda}\frac{\boldsymbol{\alpha}_i}{||\boldsymbol{\alpha}_i||}:\frac{\boldsymbol{\alpha}_i}{\sqrt{\frac{3}{2}}||\boldsymbol{\alpha}_i||}\right\rangle\frac{\boldsymbol{\alpha}_i}{\sqrt{\frac{3}{2}}||\boldsymbol{\alpha}_i||}\right) = 0
\end{aligned}
$$

The uniaxial loading behavior of this model is illustrated in Fig. 8.7, exhibiting the piecewise linear relation requiring the cumbersome judgments for the Heaviside step function in numerical calculation.

Ohno and Wang (1993) showed that the model with Eq. (8.8) exhibits similar behavior to the multi surface model. They extended Eq. (8.8) by replacing the Heaviside step function to the continuous function as follows:

$$
\overset{\circ}{\underset{i}{\boldsymbol{\alpha}}} = h_i\left[\frac{2}{3}\mathbf{d}^p - \left(\frac{\bar{a}_i}{r_i}\right)^{m_i}\left\langle \mathbf{d}^p:\frac{\boldsymbol{\alpha}_i}{\bar{a}_i}\right\rangle\frac{\boldsymbol{\alpha}_i}{r_i}\right] \ (\text{no sum}) \tag{8.11}
$$

where m_i $(i = 1, 2, \cdots, n)$ are material constants. On account of this modification, the stress vs. strain curve in the monotonic loading process becomes smooth after the stress reached the yield surface. Here, note that Eq. (8.11) for $m_i \to \infty$ is reduced to Eq. (8.8) exhibiting the bilinear curve so that the piecewise linear stress versus strain curve with the completely closed hysteresis loop resulting in a

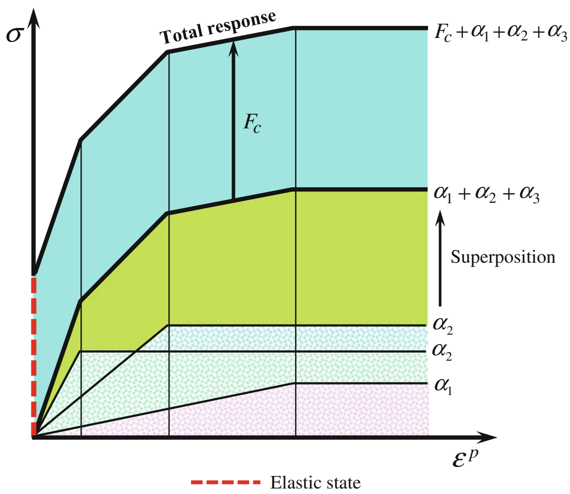

Fig. 8.7 Ohno-Wang model (Ohno and Wang 1993)

no-ratcheting is predicted. On the other hand, Eq. (8.11) for $m_i = 0$ is reduced to the Armstrong-Frederick nonlinear kinematic hardening rule so that the excessively large ratcheting is predicted. Further, the model was extended by Ohno and Abdel-Karim (2000) as follows:

$$\dot{\boldsymbol{\alpha}}_i = h_i\left(\frac{2}{3}\mathbf{d}^p - \mu_i\boldsymbol{\alpha}_i||\dot{\boldsymbol{\varepsilon}}^p|| - H[f_i]\left\langle \mathbf{d}^p : \frac{\boldsymbol{\alpha}_i}{\bar{a}_i}\right\rangle \frac{\boldsymbol{\alpha}_i}{r_i}\right) \text{ (no sum)} \tag{8.12}$$

where μ_i are the material constants. Equation (8.12) is the combination of the Armstrong-Frederick kinematic hardening and the piecewise kinematic hardening in Eq. (8.8) so that it approaches the behavior of the aforementioned Chaboche model. The Ohno model would be regarded as an impertinent modification of the Chaboche model.

The superposed kinematic hardening model possesses the following defects.

1. It is not a physical model but the empirical model due to the polynomial approximation of test data.
2. A lot of material constants without clear physical meaning are incorporated.
3. The yield surface is limited to the Mises yield surface or cylindrical yield surface in the principal stress space.
4. The tangent modulus changes suddenly from the elastic to the elastoplastic modulus at the moment when the stress reaches the yield surface, violating the smoothness condition in Eq. (7.2). Needless to say, the smooth stress-strain curve is not described but the suddenly-bent stress-strain curve is predicted. Therefore, it is required to determine the offset value, i.e. the plastic stain at yield point, which is accompanied with an arbitrariness.
5. Plastic deformation cannot be predicted for the cyclic loading inside the yield surface even in a high stress level.
6. It is physically impertinent that the small yield surface enclosing a purely-elastic domain reaches a high stress, i.e. full yield state.
7. The continuity condition in Eq. (7.1) is also violated at the moment when the stress reaches the bounding surface if the tangential inelastic strain rate is incorporated.
8. Judgment whether or not the current stress reaches the yield surface is required in the loading criterion.
9. Numerical calculation of cyclic loading behavior in the vicinity of small yield surface is unstable, the tangent modulus jumping from the elastic to the elastoplastic ones and vice versa.
10. The applicability is limited to the description of the deformation behavior for the variation of stress in the deviatoric stress plane so that it is limited to metals only with the Mises yield condition and the plastic equivalent hardening. On the other hand, the multi- and the two-surface and the subloading surface models have been applied to soils, and the multi-surface and the subloading

surface model has been further applied to friction phenomena (e.g. Mroz and Stupkiewicz 1994; Hashiguchi et al. 2005b, 2016; Hashiguchi, 2013a; Hashiguchi and Ozaki, 2008). Consequently, the superposed kinematic hardening model lacks the generality markedly.

11. The explicit formulations of this model are concerned with infinitesimal deformation up to several percent strain without a rotation, which are based on the infinitesimal strain in Eq. (2.49) possessing the deficiencies described in Sect. 2.6 and the material-time derivatives of the stress and the kinematic hardening violating the objectivity as described in Sect. 4.4. Therefore, it ignores even the fundamentals of modern continuum mechanics started by Oldroyd (1950) at the middle of the last century. Needless to say, it is inapplicable to the deformation analyses under a material rotation as seen in a metal forming process for instance. On the other hand, the other models, e.g. the subloading loading and the two surface models are formulated in the hypoelastic-based plasticity which holds for the finite deformation up to 100 % strain under a finite rotation even if the Jaumann rate is adopted.

Nevertheless, the ad hoc Chaboche model was officially implemented in the commercial software Marc and Abaqus so that it is used widely by metal engineers because it can be understood even by the beginners of elastoplasticity theory possessing the elementary knowledge only of the Mises yield condition, the kinematic hardening, the infinitesimal strain and the material-time derivative lacking the objectivity.

8.2.6 Common Drawbacks in Cyclic Kinematic Hardening Models

The cyclic plasticity models based on the kinematic hardening concept possess the common drawbacks as follows:

1. The original purpose for the creation of unconventional plasticity model is the description of the plastic strain rate by the rate of stress inside the yield surface which cannot be described by the conventional model assuming the yield surface enclosing a purely-elastic domain. The purpose cannot be attained endlessly by the methods which incorporate the small yield surface enclosing a purely-elastic domain.
2. It is premised that the development of plastic strain rate (decrease of plastic tangent modulus) proceeds by the development of the kinematic hardening. In fact, however, the main source for the development of plastic strain rate would be different from the kinematic hardening, i.e. anisotropy because the plastic

strain rate develops as the stress increases to overcome the friction resistance between material particles, i.e. as the stress approaches the yield surface. Therefore, these models would lack the physical rationality.

3. The tangent modulus lowers suddenly from the elastic one to the elastoplastic one at the yield point so that the smoothness condition in Eq. (7.2) is violated and thus a smooth stress-strain curve cannot be described. Therefore, it is required to determine the offset value, i.e. the plastic stain at yield point, which is accompanied with an arbitrariness.
4. The strain accumulation in a small cyclic loading inside a small yield surface cannot be described since a small yield surface enclosing an elastic domain is assumed. Note that even the cyclic loading in a high stress near full yield state does not cause the strain accumulation as shown in Fig. 8.8. This kind of loading situation is often observed in practical engineering, e.g. the phenomenon that the cantilever supporting a weight near yielding load is subjected to a cyclic loading with a small stress amplitude by a wind or a sea waves for instance. This defect leads to the risky mechanical design for the cyclic loading by which a large strain accumulation is induced in real materials. In addition, the spring-back phenomenon cannot be described as described for the two-surface model.
5. The judgment whether or not the stress reaches conventional-yield (outmost, bounding, limit, small yield) and/or subyield surface is fulfilled is required in the loading criterion.
6. The continuity condition in Eq. (7.1) is also violated if the tangential-inelastic strain rate is incorporated since it is induced suddenly when the stress reaches the surface(s). Therefore, the non-proportional loading behavior and the plastic instability phenomena cannot be described pertinently.

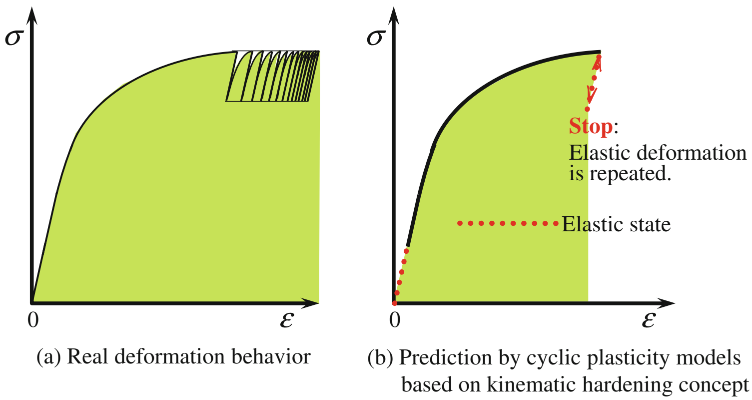

Fig. 8.8 Unrealistic prediction of cyclic loading behavior after partial unloading-reloading by the multi, the two and the superposed kinematic hardening models postulating purely elastic domain

7. The mathematical structures of these models differ basically from the conventional plasticity, assuming the plural surfaces (the multi and the two surface models) or the small yield surface (the superposed kinematic hardening model). On the other hand, the mathematical structure in the subloading surface model is the natural extension of that in the conventional one, assuming only the conventional yield surface as an independent surface as was shown in Chap. 7 and will be shown elaborately in Chap. 9.
8. Quite small loading increments must be input resulting in inefficient numerical calculation as far as any particular computer subroutine to pulled-back the stress to the yield surface (Kobayashi and Ohno, 2002; Ghaei and Green, 2010) is not incorporated, because the automatic controlling function to pull-back the stress to the yield surface contained in the subloading surface model is not furnished. Besides, numerical calculation of cyclic loading behavior in the vicinity of small yield surface is unstable, the tangent modulus jumping from the elastic to the elastoplastic ones and vice versa.
9. Phenomena which can be implemented to the return-mapping projection are limited. In fact, it would be difficult to incorporate the cyclic isotropic hardening-stagnation which will be described in Sect. 10.2 since the pull-back of the plastic strain or the back stress to the isotropic hardening surface cannot be executed readily in the return-mapping projection. It is quite peculiar that the cyclic isotropic hardening-stagnation is abandoned by the proposers themselves (Chaboche et al. 1979; Chaboche 2008; Ohno 1982; Kobayashi and Ohno 2002) in the FEM analyses.
10. The exact finite strain theory based on the multiplicative decomposition of deformation gradient, called the *multiplicative finite strain theory*, cannot be formulated for the kinematic hardening models. On the other hand, the exact formulation was attained for the subloading surface model as will be described in detail in Chap. 12.
11. They have been formulated for the description of elastoplastic deformation of pressure-independent Mises metals and thus it is difficult or impossible for these models to be applied to materials other than pressure-independent metals, e.g. pressure-dependent metals, soils, rocks and concretes. Therefore, the cyclic kinematic hardening models would be the ad hoc models which are applicable only to quite limited material and phenomena.

As known from the facts revealed in this section, the cyclic kinematic hardening models possess various serious defects. Nevertheless, they are installed widely in the commercial FEM software (Chaboche model: Marc, Abaqus; Yoshida-Uemori model: PAM-STAMP, LS-DYNA (Japan)). The proposers of the cyclic kinematic-hardening models, i.e. the multi surface, the two surface and the superposed-kinematic hardening models should accept sincerely the intrinsic limits and defects of these models and also the users of these models should recognize these serious limits and defects for the sound development of elastoplastic theory and deformation analysis.

On the other hand, the subloading surface model described in the last chapter, the next section and the subsequent chapters would be the universal model which will become widespread with the passage of time. The overall assessment of cyclic plasticity models is summarized in Table 8.1.

8.3 Expansion of Loading Surface: Extended Subloading Surface Model

The subloading surface model formulated in Chap. 7, called the *initial subloading surface model* hereinafter, is incapable of describing cyclic loading behavior appropriately, predicting an open hysteresis loop in an unloading-reloading process and thus overestimating a mechanical ratcheting phenomenon. The insufficiency is caused by the fact that the similarity-center of the normal-yield and the subloading surfaces is fixed at the origin of stress space and thus a purely-elastic deformation is described in the unloading process, resulting in the open hysteresis loop. Here, it should be noted that purely-elastic response is induced only in an initiation of reverse loading process in general. Then, the insufficiency was remedied by making the similarity-center of the normal-yield and the subloading surfaces translate with the plastic deformation (Hashiguchi 1985b, 1986, 1989).

The uniaxial loading behavior is depicted in Fig. 8.9 for the simple material behavior without a variation of the normal-yield surface. The similarity-center goes up following the stress by the plastic strain rate in the initial loading process as seen in Fig. 8.9a, b. The subloading surface shrinks and thus only elastic strain rate is induced until the stress goes down to the similarity-center in the unloading process as seen in Fig. 8.9c. After that the subloading surface begins to expand and thus the plastic strain rate in the compression is induced in the unloading-inverse loading process whilst the similarity-center goes down following the stress by the plastic strain rate as seen in Fig. 8.9d. Again only the elastic strain rate is induced until the stress goes up to the similarity-center in the reloading process from the complete unloading as seen in Fig. 8.9e. After that the subloading surface begins to expand and thus the plastic strain rate is induced whilst the similarity-center goes up following the stress by the plastic strain rate as seen in Fig. 8.9f. The expanded figure of Fig. 8.9f is also shown at the lowest part in Fig. 8.9. Consequently, the closed hysteresis loop is depicted realistically as shown in this figure.

Table 8.1 Assessment of cyclic plasticity models

<table>
<tr><th colspan="2">Cyclic plasticity models</th><th>Smoothness condition</th><th>Judgment of yielding in loading criterion</th><th>Automatic control to pull-back stress to yield surface</th><th>Description of plastic strain accumulation under cyclic loading for small strain amplitude</th><th>Continuity condition in incorporation of tangential inelastic strain rate</th><th>Applicability to materials other than Mises metals</th><th>Formulation of multiplicative finite strain theory</th></tr>
<tr><td rowspan="3">Cyclic kinematic hardening model (Translation of small yield surface)</td><td>Multi surface model (Mroz)</td><td rowspan="3">Violate</td><td rowspan="3">Necessary</td><td rowspan="3">Impossible</td><td rowspan="3">Impossible</td><td rowspan="3">Violate</td><td rowspan="2">Difficult</td><td rowspan="3">Impossible</td></tr>
<tr><td>Two surface model (Dafalias)</td></tr>
<tr><td>Superposed Kinematic hardening model (Chaboche)</td><td>Impossible</td></tr>
<tr><td>Expansion of loading surface</td><td>Subloading surface model (Hashiguchi)</td><td>Fulfills</td><td>Un-necessary</td><td>Possible</td><td>Possible</td><td>Fulfills</td><td>Applicable generally</td><td>Already formulated</td></tr>
</table>

The extended subloading surface model would describe the cyclic loading behavior realistically as illustratively shown in Fig. 8.10. It does not contain any drawbacks in the cyclic plasticity models based on the kinematic hardening concept, while the continuity and the smoothness conditions in Eqs. (7.1) and (7.2) are satisfied only in this model. Then, it has been applied to the descriptions of rate-independent and rate-dependent elastoplastic deformation behavior and plastic-instability phenomena of not only metals but also geomaterials and further the friction phenomena between solids as will be described in detail in the subsequent chapters.

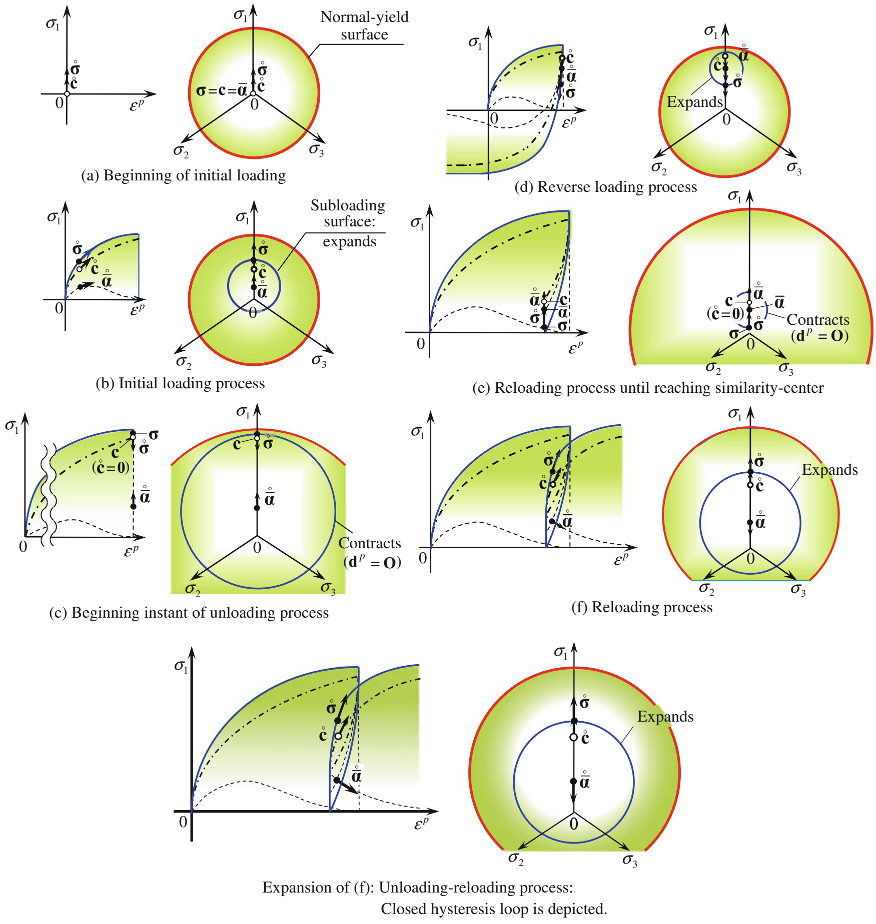

Fig. 8.9 Prediction of uniaxial loading behavior by extended subloading surface model: **a** initial state, **b** initial loading process, **c** unloading process until similarity-center, **d** unloading-inverse loading process after passing similarity-center, **e** reloading process until reaching similarity-center and **f** reloading process. (—— Stress, –·–·– Elastic-core, - - - - Center of subloading surface)

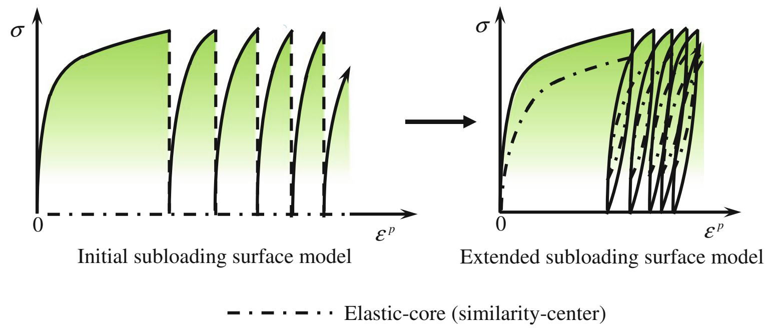

Fig. 8.10 Modification of subloading surface model to describe cyclic loading behavior

References

Armstrong PJ, Frederick CO (1966) A mathematical representation of the multiaxial Bauschinger effect. CEGB Report RD/B/N 731 (or in Materials at High Temperature 24:1–26 (2007))

Chaboche JL (2008) A review of some plasticity and viscoplasticity constitutive theories. Int J Plast 24:1642–1693

Chaboche JL, Rousselier G (1983) On the plastic and viscoplastic constitutive equations, Parts I and II. J Pressure Vessel Tech (ASME) 165:153–164

Dafalias YF, Popov EP (1975) A model of nonlinearly hardening materials for complex loading. Acta Mech 23:173–192

Dafalias YF, Popov EP (1976) Plastic internal variables formalism of cyclic plasticity. J Appl Mech (ASME) 43:645–651

Dafalias YF, Popov EP (1977) Cyclic loading for materials with a vanishing elastic domain. Nucl Eng Design 41:293–302

Chaboche JL, Dang-Van, K, Cordier G (1979) Modelization of the strain memory effect on the cyclic hardening of 316 stainless steel, Transactions on 5th international conference of SMiRT, Berlin, Division L., Paper No. L. 11/3

Ellyin F (1989) An anisotropic hardening rule for elastoplastic solids based on experimental observations. J Appl Mech (ASME) 56:499–507

Ghaei A, Green DE (2010) Numerical implementation of Yoshida-Uemori two-surface plasticity model using a fully implicit integration scheme. Compt Mater Sci 48:195–205

Hashiguchi K (1981) Constitutive equations of elastoplastic materials with anisotropic hardening and elastic-plastic transition. J Appl Mech (ASME) 48:297–301

Hashiguchi K (1985b) Subloading surface model of plasticity. In: Constitutive laws of soils (Proc. Discuss. Ses. 1A, 11th Int. Conf. Soil Mech. Found. Eng.), San Francisco, pp 127–130

Hashiguchi K (1986) Elastoplastic constitutive model with a subloading surface. In: Proceedings of international conference on computer mechanics, pp IV65–70

Hashiguchi K (1988) A mathematical modification of two surface model formulation in plasticity. Int J Solids Struct 24:987–1001

Hashiguchi K (1989) Subloading surface model in unconventional plasticity. Int J Solids Struct 25:917–945

Hashiguchi K (2013) General description of elastoplastic deformation/sliding phenomena of solids in high accuracy and numerical efficiency: subloading surface concept. Arch Compt Meth Eng 20:361–417

Hashiguchi K, Ozaki S (2008) Constitutive equation for friction with transition from static to kinetic friction and recovery of static friction. Int. J. Plasticity 24:2102–2124

Hashiguchi K, Ozaki S, Okayasu T (2005) Unconventional friction theory based on the subloading surface concept. Int J Solids Struct 42:1705–1727
Hashiguchi K, Ueno M, Kuwayama T, Suzuki N, Yonemura S, Yoshikawa N (2016) Constitutive equation of friction based on the subloading surface concept. Proc. Royal Soc., London A: 472:1–24 http://dx.doi.org/10.1098/rspa.2016.0212
Hashiguchi K, Yamakawa Y (2012) Introduction to finite strain theory for continuum elasto-plasticity, wiley series in computational mechanics. Wiley, Chichester
Hassan S, Kyriakides S (1992) Ratcheting in cyclic plasticity. Part I: uniaxial behavior. J Appl Mech (ASME) 8:91–116
Iwan WD (1967) On a class of models for the yielding behavior of continuous and composite systems. J Appl Mech (ASME) 34:612–617
Kobayashi M, Ohno N (2002) Implementation of cyclic plasticity models based on a general form of kinematic hardening. Int J Numer Meth Eng 53:2217–2238
Krieg RD (1975) A practical two surface plasticity theory. J Appl Mech (ASME) 42:641–646
Lemaitre JA, Chaboche J-L (1990) Mechanics of solid materials. Cambridge University Press, Cambridge
Masing G (1926) Eigenspannungen und Verfestigung beim Messing. In: Proceedings of the 2nd international congress of applied mechanics, Zurich, pp 332–335
McDowell DL (1985) An experimental study of the structure of constitutive equations for nonproportional cyclic plasticity. J Eng Mater Tech (ASME) 107:307–315
McDowell DL (1989) Evaluation of intersection conditions for two-surface plasticity theory. Int J Plast 5:29–50
Mroz Z (1966) On forms of constitutive laws for elastic-plastic solids. Arch Mech Stos 18:3–35
Mroz Z (1967) On the description of anisotropic workhardening. J Mech Phys Solids 15:163–175
Mroz Z (1976) A non-linear hardening model and its application to cyclic plasticity. Acta Mech 25:51–61
Mroz Z, Stupkiewicz S (1994) An anisotropic friction and wear model. Int J Solids Struct 31:1113–1131
Mroz Z, Norris VA, Zienkiewicz OC (1981) An anisotropic, critical state model for soils subject to cyclic loading. Geotechnique 31:451–469
Ohno N (1982) A constitutive model of cyclic plasticity with a non-hardening strain region. J Appl Mech (ASME) 49:721–727
Ohno N, Abdel-Karim M (2000) Uniaxial ratchetting of 316FR steel at room temperature—part II: constitutive modeling and simulation. J Eng Mater Tech (ASME) 122:35–41
Ohno N, Kachi Y (1986) A constitutive model of cyclic plasticity for nonlinearly hardening materials. J Appl Mech (ASME) 53:395–403
Ohno N, Wang JD (1993) Kinematic hardening rules with critical state of dynamic recovery, Part I: formulation and basic features for ratcheting behavior. Part II: application to experiments of ratcheting behavior. Int J Plast 9:375–403
Ohno N, Tsuda M, Kamei T (2013) Elastoplastic implicit integration algorithm applicable to both plane stress and three-dimensional stress states. Finite Elements Anal Design 66:1–11
Oldroyd JG (1950) On the formulation of rheological equations of state. Proc Roy Soc Lond A200:523–541
Prager W (1956) A new methods of analyzing stresses and strains in work hardening plastic solids. J Appl Mech (ASME) 23:493–496
Yoshida F, Uemori T (2002a) Elastic-plastic behavior of steel sheets under in-plane cyclic tension-compression at large strain. Int J Plast 18:633–659
Yoshida F, Uemori T (2002b) A model of large-strain cyclic plasticity describing the Bauschinger effect and workhardening stagnation. Int J Plast 18:661–686
Yoshida F, Uemori T (2003) A model of large-strain cyclic plasticity and its application to springback simulation. Int J Mech Sci 45:1687–1702